photonics

MDPI

Brief Report

Kerr-Lens Mode-Locked Tm,Ho:Ca(Gd,Y)AlO_4 Laser

Zhang-Lang Lin [1,2], Peixiong Zhang [3], Pavel Loiko [4], Xavier Mateos [5], Ge Zhang [2], Zhen Li [3], Zhenqiang Chen [3], Uwe Griebner [1], Weidong Chen [1,2] and Valentin Petrov [1,*]

[1] Max Born Institute for Nonlinear Optics and Ultrafast Spectroscopy, 2a Max Born Str., 12489 Berlin, Germany
[2] State Key Laboratory of Functional Crystals and Devices, Fujian Institute of Research on the Structure of Matter, Chinese Academy of Sciences, Fuzhou 350002, China
[3] Department of Optoelectronic Engineering, Jinan University, Guangzhou 510632, China
[4] Centre de Recherche sur les Ions, les Matériaux et la Photonique (CIMAP), UMR 6252 CEA-CNRS-ENSICAEN, Université de Caen, 6 Boulevard Maréchal Juin, 14050 Caen Cedex 4, France
[5] Física i Cristal·lografia de Materials (FiCMA), Universitat Rovira i Virgili (URV), 43007 Tarragona, Spain
* Correspondence: petrov@mbi-berlin.de

Abstract

We demonstrate Kerr-lens mode-locked operation of a Tm,Ho:Ca(Gd,Y)AlO_4 laser pumped by a narrow-linewidth, continuous-wave Ti:sapphire laser at 797 nm. Soliton pulses as short as 145 fs are generated at 2087.8 nm in σ-polarization via soft-aperture Kerr-lens mode-locking, with an average output power of 203 mW (0.5% output coupler) at ~80.5 MHz. To the best of our knowledge, this result represents the first demonstration of a Kerr-lens mode-locked laser based on a Tm,Ho:Ca(Gd,Y)AlO_4 crystal exhibiting both structural and compositional disorder.

Keywords: calcium rare-earth aluminates; disordered laser crystals; mixed laser crystals; Tm,Ho codoped laser crystals; Kerr-lens mode-locking; femtosecond pulses; 2 μm lasers

1. Introduction

Over the last decade, the tetragonal calcium rare-earth aluminates ($CaREAlO_4$) have established themselves as one of the most promising classes of laser host crystals for femtosecond oscillators emitting not only in the 1 μm range (Yb-doping) but also near 2 μm [1]. They are attractive due to a rare combination of properties: broadband emission bands related to their structural disorder on one side, and relatively high thermal conductivity on the other side which is nearly isotropic and insensitive to the doping-level [2], a property not typical for disordered crystals. The structure disorder in the $CaREAlO_4$ compounds originates from the statistical distribution of Ca^{2+} and RE^{3+} cations over the same Wyckoff site (4e, C_{4v}-symmetry). Notably, only two such stoichiometric crystals with the K_2NiF_4-type structure (sp. gr. $I4/mmm$) exist, with passive RE^{3+} = Y^{3+} and Gd^{3+} ions which exhibit congruent melting, i.e., they can be grown in a large volume, whereas doping with optically active RE^{3+} ions is relatively easy due to the presence of the substitutional RE site. Initial studies involving these two compounds revealed that Tm,Ho-codoping is particularly advantageous for femtosecond laser operations in the 2 μm spectral range [1,3]. The relatively weak ligand fields in $CaREAlO_4$ crystals produce only weak Stark splitting of the dopant ground state multiplet and the Tm^{3+} emission based on the quasi-three-level laser scheme with the transition to the ground state, is confined to wavelengths below 2 μm, where structured water vapor absorption severely limits the laser performance. For this reason, singly Tm-doping resulted in rather narrow spectral bandwidths and consequently relatively long pulse durations from mode-locked (ML) lasers [1,4]. Singly Ho-doping, on the other hand,

Check for updates

Received: 30 November 2025
Revised: 27 December 2025
Accepted: 30 December 2025
Published: 31 December 2025

Copyright: © 2025 by the authors. Licensee MDPI, Basel, Switzerland. This article is an open access article distributed under the terms and conditions of the Creative Commons Attribution (CC BY) license.

is very attractive for power scaling under in-band pumping to the upper laser level by Tm lasers, but the emission spectra are more structured (just like in any other host crystals), which is not optimal for the generation of the shortest pulses [5–8]. Yet, Tm,Ho codoping presents further challenges due to the energy-transfer upconversion processes from the metastable states of both active ions. In this regard, the favorable thermal properties of the calcium rare-earth aluminates provide a significant advantage for the management of the associated heat load.

While both Tm,Ho:$CaYAlO_4$ and Tm,Ho:$CaGdAlO_4$ feature broad, flat and smooth spectral gain profiles extending beyond 2 μm due to the significant inhomogeneous line broadening associated with their disordered structure, more recent advancements with these materials were driven by engineering the host composition in order to augment the inherent structural disorder with a compositional disorder. The latter is expected to additionally smooth and flatten the emission spectra, thereby facilitating the generation of yet shorter femtosecond pulses. Mixed crystals of this type with compositional disorder were first developed for Tm-doping [4,9], but more recently also for Tm,Ho-codoping. For instance, Tm,Ho:$CaGdAlO_4$ crystals were additionally doped with up to 10.8 at.% Lu [10,11] and subsequently employed in ML lasers. In [12], a laser based on a $CaGdAlO_4$ crystal codoped with 4.48 at.% Tm, 0.54 at.% Ho, and 5.51 at.% Lu, and pumped near 801 nm by a Ti:sapphire laser, was passively mode-locked by a SEmiconductor Saturable Absorber Mirror (SESAM) to produce 46 fs pulses at 2033 nm. The same crystal and pump source were also used in a laser incorporating a Single-Walled Carbon Nanotube (SWCN) saturable absorber (SA) to stabilize a soft-aperture Kerr-lens mode-locking (KLM) regime and generate yet shorter pulses of 38 fs at ~2040 nm [13]. Laser diode pumping at 793 nm of a SESAM ML laser based on this crystal has also been demonstrated [14]. In-band pumping to the Tm upper level at 1678 nm by a Raman shifted Er-fiber laser further helped to suppress thermal effects and to increase the average output power, enabling the generation of 218 fs pulses at 2071.5 nm by SESAM mode-locking [15] and 79 fs pulses at 2073.6 nm via soft-aperture KLM [16]. $CaYAlO_4$ was also doped with the passive Lu [17] and a Tm,Ho laser based on such a mixed host, in-band pumped at 1700 nm, generated 58 fs pulses at 2054 nm using a SESAM [18]. However, it is important to emphasize that since $CaLuAlO_4$ does not exist, the doping of $CaGdAlO_4$ [10,11] or $CaYAlO_4$ [4,17] with Lu is rather limited. Moreover, adding Lu to $CaYAlO_4$ is not expected to substantially increase the inhomogeneous spectral line broadening due to the similar ionic radii of Y^{3+} and Lu^{3+}.

Optimum compositional disorder in the host matrix can be expected by mixing Y and Gd in the growth melt as a complete isostructural solid-solution series of $CaGd_xY_{1-x}AlO_4$ exists for the entire range of $0 < x < 1$. A mixed host crystal of this type with Tm,Ho-codoping was used for the first time in [19] where in-band pumping at 1700 nm and SESAM mode-locking produced 50 fs pulses at 2078 nm. However, the Y and Gd mixing ratio in this work was 9:1, just as in the case of Y and Lu in [17] or the maximum Lu content achieved in $CaGdAlO_4$ in [10,11]. Note that such small amounts of the second passive component are comparable to the Tm^{3+}-doping levels, and without a direct comparison, it is difficult to attribute the improvements reported in [4,12,13,15,16,18,19] to the passive codoping ion alone, while they might have been simply related to crystalline quality. At such low concentrations, the active ion doping itself induces a similar degree of disorder, yet such crystals are not classified as compositionally disordered. Obviously, a maximum effect of compositional disorder can be expected for similar levels of Gd and Y in the passive host. Such a composition of $CaTm_{0.0336}Ho_{0.0047}Gd_{0.4230}Y_{0.5387}AlO_4$ was reported for the first time in [20]. In [21,22], we demonstrated SESAM mode-locking using this crystal under Ti:sapphire (797 nm) and in-band (1678 nm) laser pumping, achieving 114 fs pulses at 2130 nm and sub-50

fs pulses near 2100 nm, respectively. Here, we report on our first attempts to achieve KLM with this same codoped mixed crystal pumping by a Ti:sapphire laser.

2. Experimental Setup

A linear X-folded standing-wave cavity was used for evaluating the ML laser performance. The mixed codoped crystal employed was grown by the conventional Czochralski method using an [001] oriented undoped $CaYAlO_4$ seed under nitrogen atmosphere and a melt composition of $CaTm_{0.05}Ho_{0.005}Y_{0.615}Gd_{0.33}AlO_4$ [20]. The actual post growth composition was determined by Inductively Coupled Plasma Mass Spectrometry (ICP-MS) to be $CaTm_{0.0336}Ho_{0.0047}Gd_{0.4230}Y_{0.5387}AlO_4$ corresponding to a Tm^{3+} doping level of 3.36 at.% (Tm^{3+} ions density 4×10^{20} cm^{-3}) and Ho^{3+} doping level of 0.5 at.% (Ho^{3+} ions density 5.6×10^{19} cm^{-3}) [20]. An *a*-cut sample was prepared from the ϕ 40 mm × 70 mm boule after annealing. It had an aperture of 4 × 4 mm^2 and a thickness of 3 mm. The uncoated sample was mounted in a water-cooled Cu holder maintained at 12 °C and placed at Brewster's angle for σ-polarization between the two folding dichroic mirrors DM_1 (pump mirror) and DM_2, both with a radius of curvature, RoC = −100 mm, as illustrated in Figure 1. The polarized absorption and emission spectroscopy of the laser crystal was reported in [20]. Although σ-polarization showed a lower emission cross-section, this polarization was selected for the present KLM investigation based on preliminary wavelength tuning experiments in the continuous-wave (CW) regime [20]. The pump source was a CW, linearly polarized, narrow-linewidth (<1 nm), Ti:sapphire laser tuned to 797 nm (corresponding to the maximum absorption of the laser crystal) which delivered an output power of up to 4 W (or a maximum incident power of 3.73 W measured after M_1).

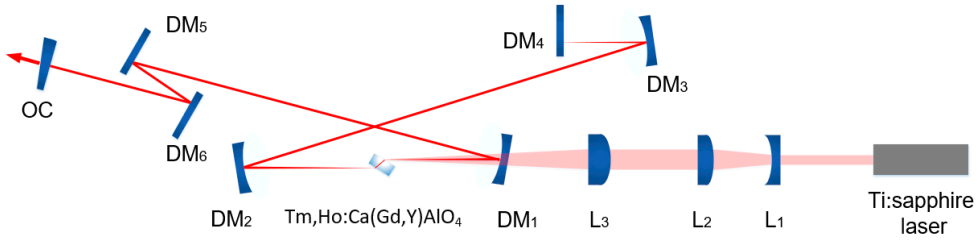


Figure 1. The experimental setup of the KLM Tm,Ho:$Ca(Gd,Y)AlO_4$ laser. L_1: negative lens (f = −50 mm); L_2: positive lens (f = 100 mm); L_3: focusing lens (f = 75 mm); DM_1–DM_3: concave dichroic dispersive mirrors; DM_4–DM_6: flat dispersive mirrors; OC: output coupler.

The pump laser beam was expanded by a telescope consisting of a plano-concave negative lens L_1 and a best shape positive lens L_2, and then focused into the laser crystal with a best shape positive lens L_3 to a beam radius (waist) of ~15 μm × ~32 μm, as shown in Figure 1. Here, the value of ~15 μm in the sagittal plane was directly measured in air by a beam-profiling camera (WinCamD, DataRay Inc., Monterey (CA), USA) with an actual resolution of 3–5 μm, while the value of ~32 μm in the tangential plane was calculated for Brewster's angle of incidence. The pump polarization was also selected to be horizontal (corresponding to σ-polarization in the laser crystal) to avoid the reflection losses under Brewster's geometry, although the absorption cross-section for this polarization is roughly two times lower [20].

The cavity group delay dispersion (GDD) was adjusted by two types of dispersive mirrors (DMs), see Figure 1: the already mentioned dichroic focusing mirrors DM_1 and DM_2, as well as the analogous mirror DM_3 which created a second cavity waist (all of them with GDD = −400 fs^2 per bounce, Layertec GmbH, Mellingen, Germany) and the flat dispersive mirrors DM_4–DM_6 (all of them with GDD = −1000 fs^2 per bounce, Ultrafast Innovations, Garching (Munich), Germany). Thus, the total round-trip cavity GDD due

to the DMs amounted to -7400 fs^2 with additional -260 fs^2 due to the laser crystal (calculated by interpolation of the Sellmeier equations for the ordinary wave in the $CaYAlO_4$ and $CaGdAlO_4$ crystals [23]). We established that such a GDD value was optimum for stable KLM with the available output couplers (OCs), although the soliton regime was not self-starting. These mirrors were specified as Tm-laser outcouplers with the actual transmission at the central laser wavelength deviating from the specifications. The latter was estimated from the measured transmission curves provided by the supplier (Layertec GmbH, Mellingen, Germany). The OCs used in the present work were wedged with an angle of 30′ to suppress parasitic etalon effects.

The second cavity waist formed near DM_4 was intentionally introduced as a geometric degree of freedom in the resonator design, rather than as an additional Kerr-active region. While the Kerr-lens responsible for mode-locking was exclusively generated inside the Tm,Ho:Ca(Gd,Y)AlO_4 crystal where the intracavity intensity is maximized, the secondary waist at DM4 was predominantly determined by linear cavity geometry and was therefore weakly sensitive to Kerr-induced mode-size variations, thus improving the robustness and reproducibility of the KLM regime. This additional cavity waist provided increased flexibility in cavity alignment and stability control, enabling fine adjustment of astigmatism compensation and cavity length while maintaining a nearly unchanged Kerr waist inside the gain crystal. In general, such an additional cavity waist permits the introduction of auxiliary intracavity elements, i.e., SESAMs for hybrid mode-locking or self-starting operation, in a spatially decoupled cavity region without perturbing the Kerr-lens strength or the mode-locking threshold. In the present experiment, it basically ensured a stable and well-controlled KLM operation by preserving the integrity of the primary nonlinear interaction region.

3. Results and Discussion

KLM operation of the Tm,Ho:Ca(Gd,Y)AlO_4 laser was first studied with a 0.8% OC (measured transmission near 2090 nm). The maximum average output power in the ML regime amounted to 278 mW for an absorbed pump power of 2.1 W (at an incident pump power of 3.1 W). Prior to achieving KLM operation, the CW output power was measured to be 225 mW which corresponded to a wavelength of ~2185 nm and a spectral width of only ~1 nm, limited by the available resolution. The transition to the ML regime was accompanied by a sudden rise in the output power, indicating a better mode-matching. To accomplish this, the separation between the two folding mirrors surrounding the laser crystal was first increased by a few hundred microns approaching the edge of the stability region. Stable KLM was then initiated by either knocking on the OC or translating the flat rear mirror DM_4.

The optical spectrum of the KLM Tm,Ho:Ca(Gd,Y)AlO_4 laser was centered at 2087.2 nm with a sech^2-fitted spectral full width at half maximum (FWHM) of 31.5 nm, see Figure 2a. A pulse duration of 152 fs (FWHM) was derived from the measured background-free second-harmonic generation (SHG) autocorrelation trace, again assuming a sech^2 intensity profile, see Figure 2b. The inset in Figure 2b shows a delay span of 15 ps indicating no satellite pulses. The corresponding time-bandwidth product (TBP) was calculated to be 0.329, only slightly above the value for ideal (unchirped) soliton pulses (0.315). The calculated peak power amounted to 20.0 kW. Figure 2c,d show the measured radio-frequency (RF) spectra over frequency spans of 1 GHz and 100 kHz, respectively. The fundamental beat note at 80.52 MHz, see Figure 2d, exhibits a very high extinction ratio of >70 dBc. The absence of any additional peaks in this figure and the constant amplitude of the harmonics in Figure 2c are further indications of stable mode-locking without any Q-switching instabilities or satellite pulses.

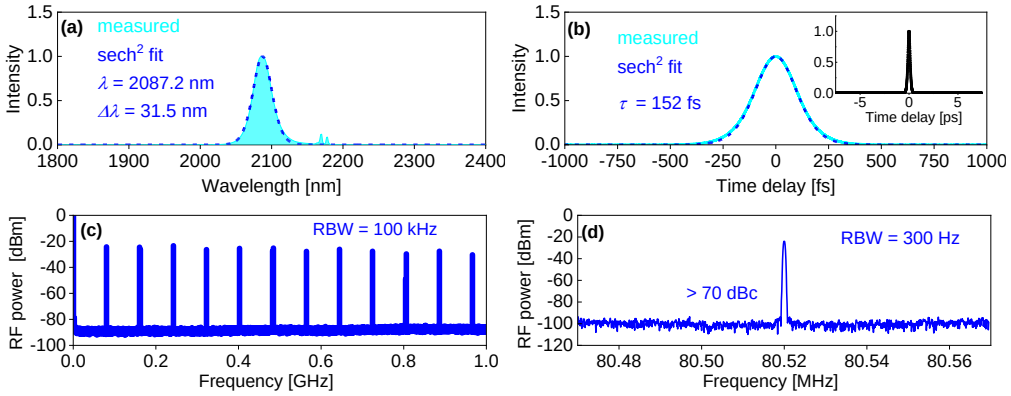


Figure 2. The recorded spectrum of the KLM Tm,Ho:Ca(Gd,Y)AlO_4 laser with a 0.8% OC (**a**), and the corresponding SHG-based noncollinear autocorrelation trace (**b**) with an inset showing a longer time span of 15 ps. Simultaneously recorded RF spectra show a 1 GHz frequency span (**c**) and the fundamental beat note on a 100 kHz span (**d**). RBW: resolution bandwidth.

A mid-IR camera (Pyrocam PY-III-C-B, Ophir-Spiricon, Andover (MA), USA) was placed at ~1.3 m from the OC to measure the far-field beam profiles when the laser operated in the CW and KLM regimes, see Figure 3a and Figure 3b, respectively. The estimated beam diameters amounted to 2.64 mm (vertical) × 2.30 mm (horizontal) in the former (Figure 3a) and to 2.30 mm (vertical) × 2.35 mm (horizontal) in the latter (Figure 3b) case, with a clear spatial change as an indication of Kerr lensing. In both regimes, the beam propagation factor M^2 was estimated to be less than 1.05 in both planes.

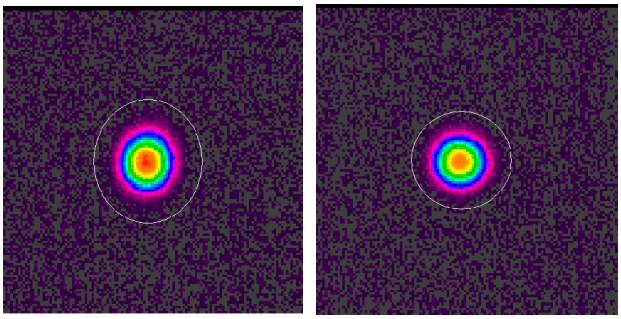


Figure 3. The recorded far field spatial profiles of the Tm,Ho:Ca(Gd,Y)AlO_4 laser output beam in the CW (**a**) and KLM (**b**) regimes using the 0.8% OC.

To achieve further pulse shortening, we employed an OC with a 0.5% measured transmission near 2090 nm. The maximum average output power in the ML regime amounted to 203 mW for an absorbed pump power of 2.2 W (at an incident pump power of 3.0 W). Prior to achieving KLM operation, the CW output power was 149 mW in this case and the wavelength was ~2087 nm. The optical spectrum of the KLM Tm,Ho:Ca(Gd,Y)AlO_4 laser was centered at a slightly longer wavelength (2087.8 nm) compared to the 0.8% OC and was also slightly broader with a FWHM of 32.2 nm assuming a $sech^2$ spectral shape, see Figure 4a. A pulse duration of 145 fs (FWHM) was derived from the measured background-free SHG autocorrelation trace, Figure 4b, again assuming a $sech^2$ intensity profile. The inset in Figure 4b shows a delay time span of 15 ps indicating again the absence of satellite pulses. The TBP with this OC was calculated to be 0.322, slightly closer to the value for ideal soliton pulses. The calculated peak power in this case amounted to 15.3 kW. Figure 4c,d show again the recorded RF spectra over frequency spans of 1 GHz and 100 kHz, respectively.

The fundamental beat note at 80.51 MHz, see Figure 4d, exhibits yet higher extinction ratio of >73 dBc and similarly, there are no indications of any instabilities or satellites.

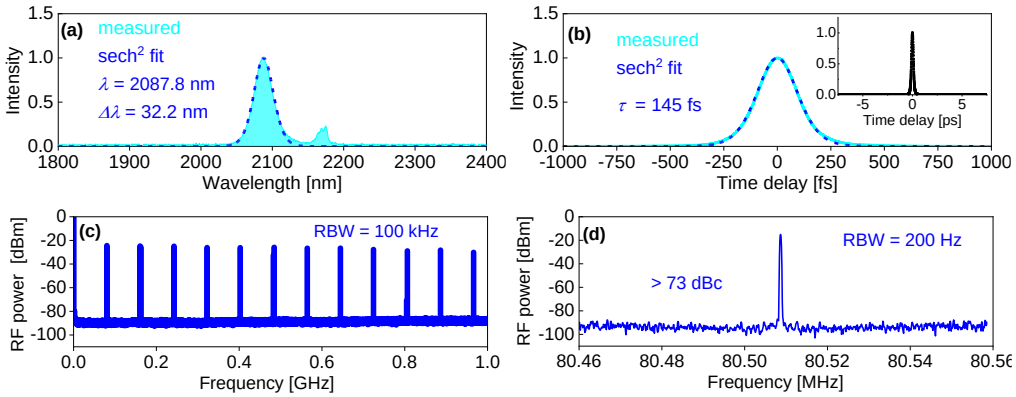


Figure 4. The recorded spectrum of the KLM Tm,Ho:Ca(Gd,Y)AlO_4 laser with a 0.5% OC (**a**), and the corresponding SHG-based noncollinear autocorrelation trace (**b**) with an inset showing a longer time span of 15 ps. Simultaneously recorded RF spectra show a 1 GHz frequency span (**c**) and the fundamental beat note on a 100 kHz span (**d**). RBW: resolution bandwidth.

The weak satellite spectral components observed in the 2150–2200 nm range in Figure 4a originate from residual intracavity GDD mismatch combined with non-optimized spectral reflectivity of the cavity mirrors in this spectral region. In the presence of strong Kerr nonlinearity and broadband mode locking, such dispersion imbalance can lead to local spectral reshaping and the appearance of secondary spectral peaks. This effect is not intrinsic to the gain medium or the Kerr-lens mode-locking mechanism itself, but rather reflects imperfect dispersion compensation over the full laser gain bandwidth. Similar short- and long-wavelength satellite features have been previously reported and systematically analyzed in SESAM and KLM Yb:$CaGdAlO_4$ lasers [24,25], where they were attributed to incomplete intracavity dispersion management at the spectral edges. We note that such spectral satellites could be effectively suppressed by optimizing the total intracavity GDD and mirror spectral phase response over the entire mode-locked pulse bandwidth, which, however, extends beyond the goal of the present work.

4. Conclusions

In conclusion, we investigated the potential of a new composition of a Tm,Ho-codoped mixed calcium rare-earth aluminate laser crystal for Kerr-lens mode-locked femtosecond operation under Ti:sapphire laser pumping. This composition was specially developed to ensure an optimum compositional disorder in addition to the inherent structural disorder to produce maximum inhomogeneous line-broadening, both in absorption and emission. Kerr-lens mode-locking has the potential of providing the shortest pulse durations and the highest average output powers due to its quasi-instantaneous temporal response and the lack of nonsaturable losses. However, the nonlinear refractive index of this composition and the entire family of such calcium aluminates is largely unknown in the 2 µm spectral range and remains to be investigated in future work. Our preliminary results achieving stable KLM operation at relatively low power levels are promising but the sub-150 fs pulse durations achieved indicate that a lot of additional efforts will be necessary to exploit the full potential of this new compositionally disordered mixed crystal towards the sub-50-fs range, as evidenced by the >240 nm wavelength tuning range demonstrated in the CW operation [20]. Apart from further optimizing the ratio of Y^{3+} to Gd^{3+} during the crystal growth process, the natural polarization selectivity should be studied as previously performed for similar crystals at normal incidence applying antireflection (AR) coatings [12].

Note that employing AR-coated samples at normal incidence may, in addition, enable cross-polarized pumping to utilize the higher absorption cross-section for the other polarization. Depending on the oscillation wavelength which in such quasi-three level laser systems is determined by the OC transmission and the overall cavity losses, such crystals may switch the polarization to a higher gain as observed in [12] near 2075 nm. While it is unclear whether the polarization having higher gain will also support larger spectral bandwidths in the ML regime, the competition between the two polarizations in this type of tetragonal crystals may prove interesting for novel active element designs utilizing an intermediate but eigen oscillating polarization inside the crystal.

Author Contributions: Conceptualization, W.C.; methodology, W.C.; software, Z.-L.L.; validation, Z.-L.L. and W.C.; formal analysis, W.C. and V.P.; investigation, Z.-L.L., P.L. and X.M.; resources, P.Z., Z.L., Z.C. and G.Z.; data curation, P.L., X.M. and U.G.; writing—original draft preparation, V.P.; writing—review and editing, V.P., W.C. and U.G.; visualization, Z.-L.L., P.Z. and P.L.; supervision, W.C.; project administration, V.P. and W.C.; funding acquisition, V.P., G.Z. and W.C. All authors have read and agreed to the published version of the manuscript.

Funding: This project has received funding from the National Natural Science Foundation of China (62475263); Science and Technology Projects of Fujian Province (2024I0041, 2023H0047); Sino-German Scientist Cooperation and Exchanges Mobility Program (DFG Grant M-0040); Ministerio de Ciencia, Innovación y Universidades (PID2022-141499OB-I00).

Data Availability Statement: Data sets generated during the current study are available from the corresponding author on reasonable request.

Conflicts of Interest: The authors declare no conflicts of interest. The authors have no relevant financial or non-financial interests to disclose. The funders had no role in the design of the study; in the collection, analyses, or interpretation of data; in the writing of the manuscript; or in the decision to publish the results.

Abbreviations

The following abbreviations are used in this manuscript:

ML	Mode-locked
SESAM	SEmiconductor Saturable Absorber Mirror
SWCN	Single-Walled Carbon Nanotube
SA	Saturable absorber
KLM	Kerr-lens mode-locking
ICP-MS	Inductively Coupled Plasma Mass Spectrometry
RoC	Radius of curvature
CW	Continuous-wave
GDD	Group delay dispersion
DM	Dispersive mirror
OC	Output coupler
FWHM	Full Width at Half Maximum
SHG	Second-harmonic generation
TBP	Time-bandwidth product
RF	Radio frequency
RBW	Resolution bandwidth

References

1. Petrov, V.; Wang, Y.; Chen, W.; Pan, Z.; Zhao, Y.; Wang, L.; Mero, M.; Choi, S.Y.; Rotermund, F.; Cho, W.B.; et al. Sub-100-fs bulk solid-state lasers near 2-micron. *Proc. SPIE* **2019**, *11209*, 112094G.
2. Georgiev, K.; Shishkov, S.; Velkov, D.; Petrov, L.; Trifonov, A.; Xu, X.; Buchvarov, I. Thermo-optical characteristics of Yb:CALYGLO for high-average-power ultrafast laser applications. In *Laser Congress 2025 (ASSL, LAC, LS&C)*; Optica Publishing Group: Washington, DC, USA, 2025; Paper JTu2A.19.
3. Wang, Y.; Loiko, P.; Zhao, Y.; Pan, Z.; Chen, W.; Mero, M.; Xu, X.; Xu, J.; Mateos, X.; Major, A.; et al. Polarized spectroscopy and SESAM mode-locking of Tm,Ho:CALGO. *Opt. Express* **2022**, *30*, 7883–7893. [CrossRef] [PubMed]
4. Dong, L.; Zhang, N.; Ding, H.; Wang, P.; Liu, Y.; Wang, Z.; Liu, J.; Zhao, Y.; Liu, S.; Xu, X.; et al. Femtosecond pulse generation from a Tm:CaYLuAlO$_4$ laser employing a birefringent filter as wavelength selector. *Appl. Phys. B* **2023**, *129*, 114. [CrossRef]
5. Yao, W.; Wang, Y.; Tomilov, S.; Hoffmann, M.; Ahmed, S.; Liebald, C.; Rytz, D.; Peltz, M.; Wesemann, V.; Saraceno, C.J. 8.7-W average power, in-band pumped femtosecond Ho:CALGO laser at 2.1 μm. *Opt. Express* **2022**, *30*, 41075–41083. [CrossRef] [PubMed]
6. Yao, W.; Wang, Y.; Ahmed, S.; Hoffmann, M.; van Delden, M.; Musch, T.; Saraceno, C.J. Low-noise, 2-W average power, 112-fs Kerr-lens mode-locked Ho:CALGO laser at 2.1 μm. *Opt. Lett.* **2023**, *48*, 2801–2804. [CrossRef] [PubMed]
7. Yao, W.; Khalili, M.; Wang, Y.; Hoffmann, M.; van Delden, M.; Musch, T.; Saraceno, C.J. GHz repetition rate, sub-100-fs Ho:CALGO laser at 2.1 μm with watt-level average power. *Opt. Lett.* **2024**, *49*, 1591–1594. [CrossRef] [PubMed]
8. Wang, J.; Yao, W.; Liu, J.; Xu, X.; Xu, J.; Leng, Y. Kerr-lens mode-locked Ho:CALYO laser at 2.1 μm. *Opt. Express* **2025**, *33*, 18017–18023. [CrossRef] [PubMed]
9. Pan, Z.; Loiko, P.; Serres, J.M.; Kifle, E.; Yuan, H.; Dai, X.; Cai, H.; Wang, Y.; Zhao, Y.; Aguilo, M.; et al. "Mixed" Tm:Ca(Gd,Lu)AlO$_4$—A novel crystal for tunable and mode-locked 2 μm lasers. *Opt. Express* **2019**, *27*, 9987–9995. [CrossRef] [PubMed]
10. Pan, Z.; Loiko, P.; Slimi, S.; Yuan, H.; Wang, Y.; Zhao, Y.; Camy, P.; Dunina, E.; Kornienko, A.; Fomicheva, L.; et al. Tm,Ho:Ca(Gd,Lu)AlO$_4$ crystals: Crystal growth, structure refinement and Judd-Ofelt analysis. *J. Lumin.* **2022**, *246*, 118828. [CrossRef]
11. Pan, Z.; Loiko, P.; Serres, J.M.; Yuan, H.; Wang, Y.; Wang, L.; Zhao, Y.; Solé, R.M.; Aguiló, M.; Díaz, F.; et al. Tm,Ho:Ca(Gd,Lu)AlO$_4$ crystals: Polarized spectroscopy and laser operation. *J. Lumin.* **2023**, *257*, 119638. [CrossRef]
12. Wang, L.; Chen, W.; Zhao, Y.; Loiko, P.; Mateos, X.; Guina, M.; Pan, Z.; Mero, M.; Griebner, U.; Petrov, V. Sub-50 fs pulse generation from a SESAM mode-locked Tm,Ho-codoped calcium aluminate laser. *Opt. Lett.* **2021**, *46*, 2642–2645. [CrossRef] [PubMed]
13. Wang, L.; Chen, W.; Pan, Z.; Bae, J.E.; Rotermund, F.; Loiko, P.; Mateos, X.; Zhang, G.; Griebner, U.; Petrov, V. Kerr-lens mode-locked Tm,Ho:Ca(Gd,Lu)AlO$_4$ laser. In *Laser Congress 2023 (ASSL, LAC)*; Optica Publishing Group: Washington, DC, USA, 2023; Paper SD1.4.
14. Tian, B.; Zhao, Y.; Zhao, S.; Liu, Y.; Li, T.; Hu, P.; Mao, J.; Yang, K.; Wang, C.; Mei, C.; et al. Harmonic mode-locking based on Tm,Ho:Ca(Gd,Lu)AlO$_4$ laser near 2.1 μm wavelength region. *Opt. Mater.* **2024**, *149*, 114990. [CrossRef]
15. Zeng, H.; Xue, W.; Murray, R.T.; Chen, W.; Pan, Z.; Wang, L.; Cui, C.; Loiko, P.; Mateos, X.; Griebner, U.; et al. Continuous-wave and mode-locked operation of an in-band pumped Tm,Ho,Lu:CaGdAlO$_4$ laser. *Appl. Sci.* **2023**, *13*, 12927. [CrossRef]
16. Zeng, H.-J.; Xue, W.-Z.; Murray, R.T.; Cui, C.; Wang, L.; Pan, Z.; Loiko, P.; Mateos, X.; Yuan, F.F.; Zhang, G.; et al. In-band pumped Kerr-lens mode-locked Tm,Ho-codoped calcium aluminate laser. *Opt. Express* **2024**, *32*, 16083–16089. [CrossRef] [PubMed]
17. Wang, P.; Jin, Y.; Lv, J.; Zhang, N.; Xue, M.; Li, K.; Dong, L.; Liu, J.; Zhao, Y.; Xu, X.; et al. Spectroscopy and efficient laser performances of a Tm,Ho:CaY$_{0.9}$Lu$_{0.1}$AlO$_4$ crystal. *Opt. Lett.* **2023**, *48*, 4544–4547. [CrossRef] [PubMed]
18. Liu, S.; Wang, P.; Li, K.; Lv, J.; Jin, Y.; Xu, X.; Wang, Z.; Liu, J.; Liu, J.; Zhao, Y. Sub-60-fs mode-locked Tm,Ho:CaYLuAlO$_4$ laser at 2.05 μm. *Opt. Express* **2024**, *32*, 7513–7519. [CrossRef] [PubMed]
19. Ding, H.; Liu, J.; Wang, Y.; Zhang, N.; Wang, Z.; Zhao, Y.; Xu, X.; Xue, Y.; Xu, J.; Griebner, U.; et al. Mode-locking of a Tm,Ho:CALYGO laser delivering 50 fs pulses at 2.08 μm. *Opt. Lett.* **2023**, *48*, 6267–6270. [CrossRef] [PubMed]
20. Zhang, P.; Lin, Z.-L.; Loiko, P.; Eremeev, K.; Li, Z.; Chen, Z.; Zhang, G.; Mateos, X.; Camy, P.; Braud, A.; et al. Growth, spectroscopy and laser operation of a "mixed" calcium aluminate Tm,Ho:Ca(Gd,Y)AlO$_4$. In *Laser Congress 2024 (ASSL, LAC, LS&C)*; Optica Publishing Group: Washington, DC, USA, 2024; Paper JTu2A.16.
21. Lin, Z.-L.; Petrov, V.; Griebner, U.; Zhang, G.; Zhang, P.; Li, Z.; Chen, X.; Mateos, X.; Loiko, P.; Chen, W. SESAM mode-locked Tm,Ho:Ca(Gd,Y)AlO$_4$ laser at 2130 nm. In Proceedings of the 13th Advanced Lasers and Photon Sources Conference (ALPS2024), Yokohama, Japan, 22–26 April 2024. Paper ALPS7-01.
22. Lin, Z.-L.; Chen, W.; Zhang, G.; Zhang, P.; Li, Z.; Chen, Z.; Murray, R.T.; Loiko, P.; Eremeev, K.; Mateos, X.; et al. Sub-50-fs in-band pumped Tm,Ho-codoped "mixed" calcium aluminate laser. In Proceedings of the Conference on Lasers and Electro-Optics (CLEO) 2025, Long Beach, CA, USA, 4–9 May 2025; Optica Publishing Group: Washington, DC, USA, 2025. Paper SS157-4.

23. Loiko, P.; Becker, P.; Bohaty, L.; Liebald, C.; Peltz, M.; Vernay, S.; Rytz, D.; Serres, J.M.; Mateos, X.; Wang, Y.; et al. Sellmeier equations, group velocity dispersion, and thermo-optic dispersion formulas for $CaLnAlO_4$ (Ln = Y, Gd) laser host crystals. *Opt. Lett.* **2017**, *42*, 2275–2278. [CrossRef] [PubMed]
24. Zaouter, Y.; Didierjean, J.; Balembois, F.; Leclin, G.L.; Druon, F.; Georges, P.; Petit, J.; Goldner, P.; Viana, B. 47-fs diode-pumped Yb^{3+}:$CaGdAlO_4$ laser. *Opt. Lett.* **2006**, *31*, 119–121. [CrossRef] [PubMed]
25. Sévillano, P.; Georges, P.; Druon, F.; Descamps, D.; Cormier, E. 32-fs Kerr-lens mode-locked Yb:$CaGdAlO_4$ oscillator optically pumped by a bright fiber laser. *Opt. Lett.* **2014**, *39*, 6001–6004. [CrossRef] [PubMed]

Disclaimer/Publisher's Note: The statements, opinions and data contained in all publications are solely those of the individual author(s) and contributor(s) and not of MDPI and/or the editor(s). MDPI and/or the editor(s) disclaim responsibility for any injury to people or property resulting from any ideas, methods, instructions or products referred to in the content.